

The Aleutian Low, storm tracks, and winter climate variability in the Bering Sea

S.N. Rodionov^a, N.A. Bond^{a,*}, J.E. Overland^b

^aJoint Institute for the Study of the Atmosphere and Oceans, Box 354235, University of Washington, Seattle, WA 98195-4235, USA

^bNOAA/Pacific Marine Environmental Laboratory, 7600 Sand Point Way NE, Seattle, WA 98115-6349, USA

Received in revised form 26 January 2007; accepted 1 August 2007

Available online 18 October 2007

Abstract

Previous studies have found inconsistent results regarding how wintertime conditions in the Bering Sea relate to variations in the North Pacific climate system. This problem is addressed through analysis of data from the NCEP/NCAR Reanalysis for the period 1950–2003. Composite patterns of sea-level pressure, 500 hPa geopotential heights, storm tracks and surface air temperature are presented for four situations: periods of strong Aleutian Low, weak Aleutian Low, warm Bering Sea air temperatures, and cold Bering Sea air temperatures. Winter temperatures in the Bering Sea are only marginally related to the strength of the Aleutian Low, and are much more sensitive to the position of the Aleutian Low and to variations in storm tracks. In particular, relatively warm temperatures are associated with either an enhanced storm track off the coast of Siberia, and hence anomalous southerly low-level flow, or an enhanced storm track entering the eastern Bering Sea from the southeast. These latter storms do not systematically affect the mean meridional winds, but rather serve to transport mild air of maritime origin over the Bering Sea. The leading indices for the North Pacific, such as the NP and PNA, are more representative of the patterns of tropospheric circulation and storm track anomalies associated with the strength of the Aleutian Low than patterns associated with warm and cold wintertime conditions in the Bering Sea.

© 2007 Elsevier Ltd. All rights reserved.

Keywords: Aleutian Low; Bering Sea; Climate variability; North Pacific; Storm tracks; Winds

1. Introduction

The Aleutian Low is a climatic feature centered near the Aleutian Islands on charts of mean sea-level pressure (SLP). It represents one of the main “centers of action” in the atmospheric circulation of the Northern Hemisphere. The Aleutian Low is most intense (lowest pressure) during the winter and

practically disappears during the summer. It is important to underscore that the Aleutian Low is a statistical feature, a result of averaging of individual synoptic maps that mark the location where traveling cyclones usually reach maximum intensity over a given averaging period (for example, a month). The intensity and geographical position of the Aleutian Low vary greatly from month-to-month, year-to-year, and even decade-to-decade (Overland et al., 1999). This variability has been assumed to exert significant influence on winter climatic conditions in the Bering Sea; however, the

*Corresponding author. Tel.: +1 206 526 6459;
fax: +1 206 526 6485.

E-mail address: nicholas.bond@noaa.gov (N.A. Bond).

mechanism explaining this influence is not well understood even on the qualitative level. Previous studies have suggested that anomalously warm winters in the Bering Sea tend to be associated with a strong Aleutian Low (Niebauer, 1983; Niebauer et al., 1999; Luchin et al., 2002), which is usually explained by a tendency of individual storm systems to preferentially pump warm air poleward (Stabeno et al., 2001). The relationship, however, is far from perfect because there have been many mild winters, such as those in the late 1960s, that occurred when the Aleutian Low was weak (McLain and Favorite, 1976). The role of the Aleutian Low in formation of anomalously cold winters in the Bering Sea is even less well understood, although there is a tendency for those winters to be associated with a weak Aleutian Low and an anomalous upper atmospheric ridge over the central North Pacific (Niebauer, 1988).

It is possible that the relationships between the severity of winters in the Bering Sea and the strength of the Aleutian Low vary with time scale. On the multi-decadal scale, the Bering Sea appears to respond to changes in the state of the Aleutian Low. In fact, when the climate of the North Pacific shifted from a regime of a weak Aleutian Low in the 1940s through the late 1970s to a regime of a strong Aleutian Low thereafter, the background temperature in the Bering Sea increased (Wooster and Hollowed, 1995). This relationship, however, does not hold for the entire spectrum of observations, at least in its simple linear form. The correlation coefficients between the North Pacific (NP) index, which measures the overall strength of the Aleutian Low, and Bering Sea ice cover or surface air temperature (SAT) are not statistically significant (Rodionov et al., 2005).

Several studies have examined the relationship of the Bering Sea climate with the geographical position of the Aleutian Low. Rogers (1981) notes that Bering Sea ice extends farther south and St. Paul of the Pribilof Islands is colder, when the Aleutian Low is farther east and deeper than normal. According to Luchin et al. (2002), anomalously cold winters occur when the Aleutian Low is displaced eastward of its normal position, irrespective of its strength. This is inconsistent with Niebauer (1988), who relates anomalously cold winters to a weakening and retreat of the Aleutian Low toward the west-northwest, as during La Niña events.

Similar inconsistency exists for anomalously warm winters in the Bering Sea. Luchin et al. (2002) found that during warm winters the Aleutian Low was not only about 3–6 hPa deeper than average, but its center is shifted 3–6° north and 10–20° west of its long-term mean position. On the other hand, Niebauer (1988) linked anomalously warm winters with El Niño events, when the Aleutian Low was both deeper than normal and shifted east of its long-term mean position. It should be noted that at least part of the association between warm winters in the Bering Sea and eastward shift of the Aleutian Low can be explained by the internal correlation between the Aleutian Low central pressure and its east–west position ($r = 0.52$), with lower central pressures associated with locations farther east (Overland et al., 1999). Later, Niebauer (1998) found that if the Aleutian Low shifted too far to the east (as during some strong El Niño events especially after the regime shift of 1977), the anomalous low-level winds over the Bering Sea were from the east and north off Alaska, resulting in above-normal ice conditions.

Apparently, winter thermal conditions in the Bering Sea are very sensitive to the position of the Aleutian Low and associated ridges and troughs in the mid-troposphere. McLain and Favorite (1976) showed that both the anomalously warm winters in the late 1960s and cold winters in the early 1970s occurred when the Aleutian Low was weak, but the mid-tropospheric ridges were positioned somewhat differently. Mock and Patrick (1998) classified 13 major atmospheric circulation patterns relevant to SAT anomalies in Beringia. Their North-Central Pacific negative and North-East Pacific negative types feature a strengthened Aleutian Low positioned just a few degrees apart. Nevertheless, while the former is associated with generally warmer-than-normal temperatures throughout most of Beringia, the latter has positive SAT anomalies only over Alaska and negative anomalies over Siberia and the Bering Sea.

Overland and Pease (1982) examined the relationship between interannual variations in Bering Sea maximum sea-ice extent and Pacific storm tracks. They found that sea-ice extent in a given winter appears to be primarily controlled by the tracks of storms entering the Bering Sea and to a lesser extent by the number of storms. In years of greatest ice extent, fewer storms enter the region, and low-pressure centers are quasi-stationary in the western

Gulf of Alaska and southeastern Bering Sea. In the light ice years, more storms propagate up the Siberian side of the Bering Sea. This exposes the ice to warm, moist air from the Pacific, drives the ice northward to the limits of the internal pack strength, and closes the polynya growth regions. Overland and Pease (1982) came to the conclusion that meteorological steering of cyclones, which is mostly external to the Bering Sea, is the primary factor in determining the interannual variability of sea-ice extent.

Rodionov et al. (2005) confirmed the results of Overland and Pease (1982) and showed that there are two major types of atmospheric circulation (W1 and C1), which can explain 51% of anomalously warm and 37% of cold winter months, respectively. It is important to underscore that the definition of types W1 and C1 is very simple and involves only the geographic position of the Aleutian Low. Type W1 is defined as an Aleutian Low, with a single center located north of 51°N and between 156°W and 173°W. Type C1 is a split Aleutian Low, with its western center located south of 52°N and the eastern center positioned not farther east than 140°W. Despite these simple definitions, the degrees of purity of the associations between these circulation types and three equally populated classes of SAT in the Bering Sea are very high. During the period 1916–2005, of 69 months with W1 type of circulation, 50 months (or 72%) were anomalously warm, 19 (18%) were near normal; there were no anomalously cold months at all. Similarly, of 63 months with C1 circulation type, 40 (64%) were anomalously cold, 12 (19%) were near normal, and only 4 (6%) were anomalously warm. In addition to the W1 and C1 types, there are other, less frequent types of atmospheric circulation for anomalously warm (types W2–W5) and cold (types C2–C5) winter months for the Bering Sea.

This work is an attempt to resolve significant ambiguities in the relationships linking severity of winters in the Bering Sea with the Aleutian Low and storm tracks, and to improve understanding of the influence of the North Pacific on the Bering Sea on interannual and multidecadal time scales. The paper is organized as follows. After describing the data and storm counting procedure, the major climatological features of atmospheric circulation and storm tracks in the North Pacific are discussed briefly. Since there are indications that the role of the Aleutian Low in the Bering Sea can change

depending on the Pacific climate regime (Niebauer, 1998), the regimes and timing of their shifts in the North Pacific and Bering Sea are examined. Atmospheric circulation patterns during periods of strong and weak Aleutian Low are compared with those for anomalously warm and cold winters in the Bering Sea. The major findings are that storms entering the Bering Sea typically follow either a Siberian or a Alaskan track, their relative frequency changes depending on the Pacific climate regime, and that the strength of the relationship between the northerly winds over the Bering Sea and the severity of its winters also changes from one regime to another.

2. Data and methods

The source of data for SLP, 500-hPa geopotential height, and SAT composite maps is the National Center for Environmental Prediction (NCEP)–National Center for Atmospheric Research (NCAR) reanalysis dataset (Kalnay et al., 1996). The storm track data were obtained from the Climate Diagnostic Center (CDC). The storm tracks were generated from the six-hourly NCEP–NCAR reanalysis SLP dataset using the algorithm discussed in Serreze (1995) and Serreze et al. (1997). Based on this dataset we calculated storm density and preferred direction of storms using $2^\circ \times 2^\circ$ grids for the area 25–75°N, 120°E–120°W.

There are a number of uncertainties associated with the mapping of cyclone frequencies and storm track densities (Zolina and Gulev, 2002). These uncertainties can be introduced by using latitude–longitude grid cells, with subsequent application of latitude-dependent correction to achieve area normalization. Hayden (1981a) listed the disadvantages of this technique and recommended using either raw frequencies (without any correction) or equal-area grids. The use of raw frequencies is justifiable for a limited latitudinal range, say 25°–45°N as in Hayden (1981b), for which the latitudinal change in area of a latitude–longitude box is less than 25%. At high latitudes, cyclone frequency becomes very sensitive to the cell size. In Arctic cyclone climatologies, therefore, it is a common practice to use an equal-area grid based on the Lambert polar stereographic projection, when the grid cells are referenced to the Cartesian coordinate system (e.g., Serreze, 1995). At lower latitudes, however, the actual configuration of cells of such grids becomes very different from that

at high latitudes and may not necessarily provide an effective detection of cyclones (Zolina and Gulev, 2002). Taylor (1986) demonstrated that it is impossible to make a simple correction for the latitudinal variation in grid cell size because cyclone frequencies depend not only on how many storm tracks are found in a region but also on the direction that the storms are traveling. For example, if the storm tracks are oriented from the southwest to the northeast, the cyclone frequency is larger by a factor of $\sqrt{2}$ compared with the case when storms are passing the same grid cell from east to west, even if the storm density remains the same. Taylor (1986) introduced a method for calculating an effective cross section given the angular distribution of storm track density.

In this work, the calculated storm track density, unlike the cyclone frequency, is essentially independent of grid cell size and shape. It is defined here as the effective number of tracks intercepted by a unit square cell, when each track is weighed inversely proportional to the length of the effective cross section Δl , which is calculated as

$$\Delta l = |\sin \alpha| + |\cos \alpha|,$$

where α is the angle at which the storm crosses a side of the cell. When the storms come perpendicular to a side of the cell, i.e., from west, east, north or south, their weight is equal to one. When a storm track is perpendicular to the cell's diagonal, its weight is reduced by a factor of $1/\sqrt{2} = 0.71$. We use square cells with side length equal to 2° latitude. Hence, our storm track density is measured in numbers of storms per 222 km of linear distance perpendicular to the preferred direction of storms in the cell and referred to the location of the center of the cell. Since the storm density is calculated for each grid point on the 2° latitude by 2° longitude mesh, the cells at the higher latitude had a greater degree of overlap, which provided some additional spatial smoothing.

3. Results and discussion

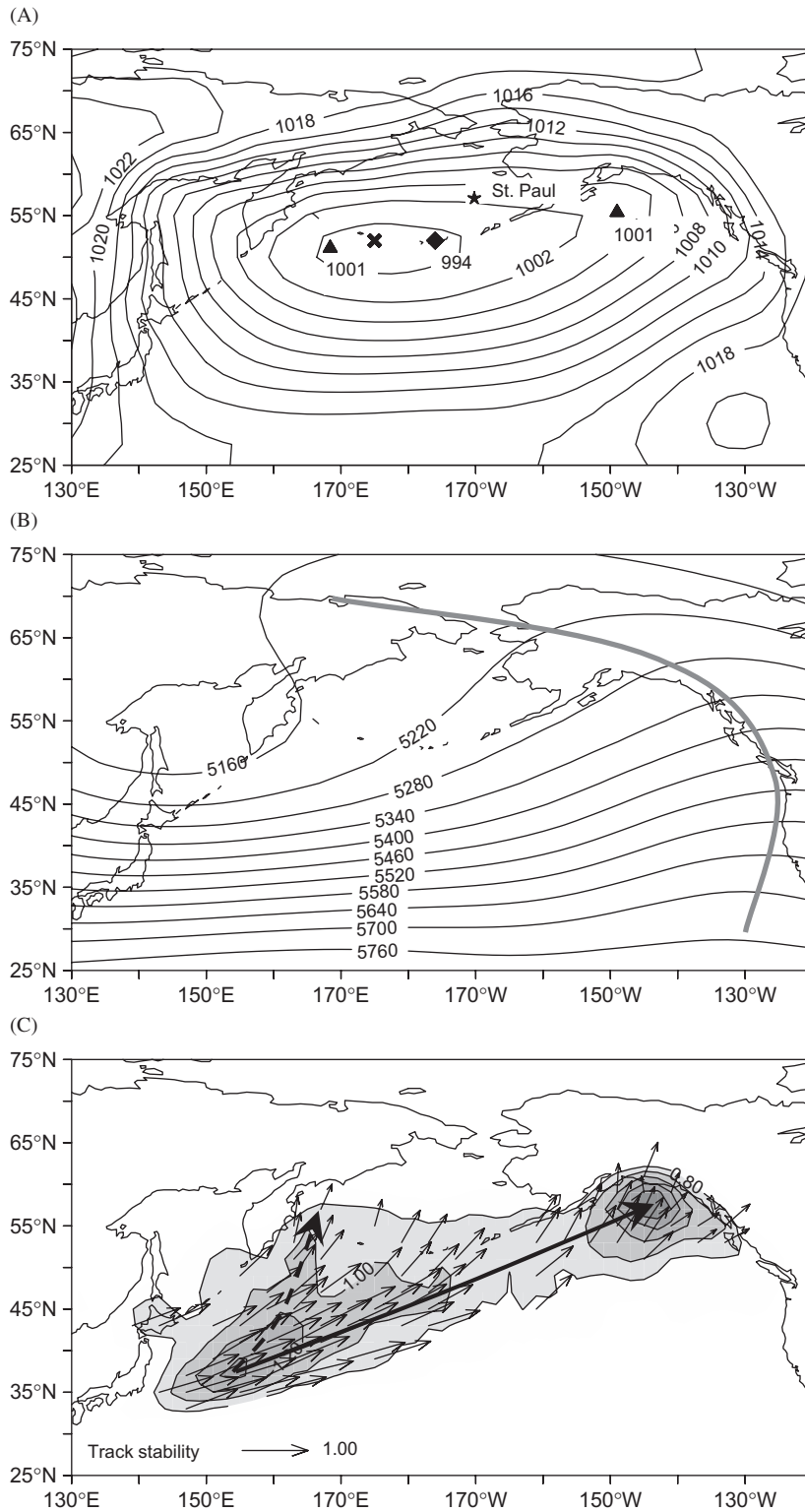
3.1. Climatological mean conditions

The mean wintertime position of the Aleutian Low is about 52°N , 175°E (Fig. 1A), based on the average winter (DJFM) distribution of SLP for the period 1951–2000. Another way to calculate the

mean position of the Aleutian Low would be to average over all realizations of its coordinates taken from each mean monthly map of the season. It turns out, however, that on about 40% of those monthly maps the Aleutian Low is split into two centers, the mean positions of which are marked by triangles in Fig. 1A. The splitting usually happens when the Aleutian Low is weak. On average, these two centers have the same SLP, and there are equal chances for one of those centers to be stronger than the other. This means that if the Aleutian Low is required to have a single center by definition, the variability of its geographic position would be greatly increased during regimes when it was weak. When the Aleutian Low is strong it usually consists of single, well-defined center. In these situations, its average location is at 52°N , 176°W , that is, 9° east of its overall mean position. Therefore, the Aleutian Low tends to be farther east when it is stronger.

The mean 500-hPa height map (Fig. 1B) characterizes the atmospheric circulation at the mid-tropospheric level. It features a climatological trough along the East Asian coast that extends into the North Pacific, and a ridge along the west North American coast. Both the trough and the ridge are quasi-stationary because their position is determined to a large extent by the Earth's orography and geographic configuration of the oceans and continents. Other variable factors such as internal atmospheric dynamics, remote influences (particularly in association with ENSO), and boundary conditions such as surface temperature and the distribution of snow and ice cause significant interannual and longer-term variations in both the positions and strengths of the East Asian trough and North American ridge. The position of the latter appears to play an especially important role in the steering of cyclones in the vicinity of the Bering Sea.

North Pacific cyclones typically originate east of Japan, over the Kuroshio Current (Gulev et al., 2001). Hoskins and Valdes (1990) point out that warm western boundary currents may play an important role in maintaining storm tracks during winter. Over 90% of the cyclones intensify after they pass through the region of the Kuroshio Current (Gyakum et al., 1989). This region is also a center of high storm track density (Fig. 1C). These storms tend to deepen and move northeastward where they frequently reach full maturity near the dateline, forming a statistical center of the Aleutian Low (marked by a cross in Fig. 1A). As mature cyclones



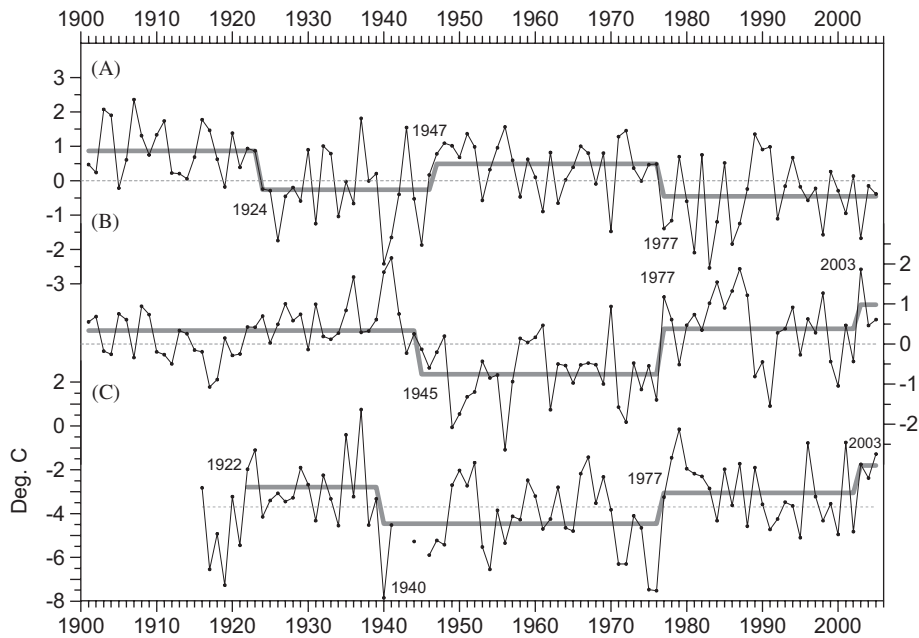


Fig. 2. Mean winter (DJFM) (A) North Pacific index, 1901–2005, (B) Pacific Decadal Oscillation index, 1901–2005, and (C) surface air temperature at St. Paul, 1916–2005. Bold gray lines characterize regime shifts calculated using the sequential method (Rodionov, 2004) with the threshold significance level $p = 0.1$ and cut-off length $l = 20$ years.

enter the eastern Pacific they track primarily into the Gulf of Alaska, where they gradually spin down. Although the Gulf of Alaska is a major graveyard for storms, cyclogenesis also occurs there several times per month from late autumn to early spring (Gyakum et al., 1989). Storm track density in this region is the highest for the North Pacific. Fig. 1C also shows the secondary path of North Pacific storms along the Siberian coast. Winters in the Bering Sea tend to be anomalously warm when this storm track is active (Overland and Pease, 1982).

3.2. Regime shift analysis

One of the most popular indices for the overall strength of the Aleutian Low is the North Pacific (NP) index (Trenberth and Hurrell, 1994). When the

NP index is positive it means that the Aleutian Low is weak, and when it is negative the Aleutian Low is strong. A regime shift analysis of the NP index (as well as of two other variables described below) was performed using the sequential method (Rodionov, 2004), with the threshold significance level $p = 0.1$ and cut-off length $l = 20$ years. The threshold significance level guarantees that the shifts between the regimes of l years in length or longer detected by the method will be significant at least at this level. The cut-off length filters out the regime shifts less than l years and is similar to the 100% cut-off point in signal filtering. As seen in Fig. 2A over the past 100+ years there were two multidecadal regimes of a weak Aleutian Low (1901–1923 and 1947–1976) and two regimes of a strong Aleutian Low (1924–1946 and 1977–2005). The actual significance level between these regimes based on

Fig. 1. Mean winter (DJFM) (A) SLP, (B) 500-hPa height, and (C) storm track density (contours) and direction (light arrows) averaged for the period 1951–2000. The minimum SLP is marked by an \times . The mean position of the Aleutian Low for nonsplit cases is marked by a diamond. The mean positions of the low pressure centers for split cases of the Aleutian Low are marked by triangles. The heavy gray line in the middle panel marks the position of the North American ridge. The length of light arrows on the bottom panel indicates storm track stability in the corresponding “square”. If all the tracks in the square are in the same direction, the arrow will have a unit length. Arrows are drawn only if the unsmoothed storm track density in the square is one or greater. Storm track density contours are smoothed by the box filter with the 1-2-1 weights, and only the contours that are 0.8 or greater are drawn. Heavier arrows indicate the primary (solid) and secondary (dashed) storm tracks.

the two-tail Student *t*-test is less than 0.005. The overall downward trend in the index is noteworthy; the level of cyclonic activity since the 1977 regime shift is, on average, the strongest over the record.

The NP index is related to the Pacific decadal oscillation (PDO), which was introduced by Mantua et al. (1997) and is based on an empirical orthogonal function (EOF) analysis of sea-surface temperature (SST) in the North Pacific, north of 20°N. The 1977 regime shift in the PDO index coincides with that in the NP index, the 1945 shift in the PDO almost coincides, and there was no statistically significant shift in the 1920s similar to that in the NP index. Nevertheless, the PDO index is predominantly positive for the period 1922–1944. It is not clear whether this disagreement between the NP and PDO indices in the earlier part of the record is the result of a lower-quality data or the large-scale ocean–atmosphere interaction being different at that time than in the more recent period. The correlation coefficients between the NP and PDO indices are -0.50 for the period 1901–1939 and -0.72 for 1940–2005.

The Bering Sea climate shifted from the cold regime of 1940–1976 to a warm regime thereafter (Fig. 2C). Another warm regime was observed in 1922–1939. There is much uncertainty in the timing of the shift from that warm regime to the next cold regime due to the lack of reliable data during World War II. The potential shift in 2003 is not discussed here, since only a few years of data are available since then.

Apparently, the Bering Sea reacts to shifts in the North Pacific climate, being in a warmer (colder) state during the regimes of a strong (weak) Aleutian Low. The slightly negative correlation coefficient between SAT at St. Paul and NP index for the period 1947–2005 covering the last two regimes in the index ($r = -0.19$) reflects this fact. When the stepwise trend is removed, however, the correlation coefficient between these two variables drops to virtually zero. It indicates that factors other than just the strength of the Aleutian Low are more important to the winter temperature in the Bering Sea.

3.3. Strong vs. weak Aleutian Low

The composite maps for a strong (low NP index values) and weak (high NP index values) Aleutian Low are presented in Figs. 3 and 4, respectively. Note that, of the 10 years with the lowest NP index since 1950, only two occurred before the regime

shift in 1977. In contrast, only two of 10 years with the highest NP index values occurred after the 1977 regime shift. Additionally, six of these 10 years were El Niño winters, and of the other four, none were La Niña winters.

When the Aleutian Low strengthens, it shifts to the east and somewhat to the south of its mean position (Fig. 3A). A stronger Aleutian Low does not necessarily mean that the number of storms increases. Gulev et al. (2001) found a statistically significant negative trend in the total number of cyclones over the North Pacific for the period 1958–1999. Meanwhile, deep cyclones (with the central pressure below 980 hPa) show a weak positive trend for the same period. The south-eastward shift of the Aleutian Low is clearly seen in Fig. 3B in terms of the negative SLP anomalies centered south of the Alaska Peninsula. This location coincides with the area of highest variability in SLP (not shown).

At the mid-tropospheric level, there is a stronger and eastward extended Asian trough and stronger than normal ridge over the west coast of North America (Fig. 3C). This eastward extension of the Asian trough is consistent with the well-known eastward extension of the Pacific jet stream during El Niño years, when the Aleutian Low tends to be stronger than normal (e.g., Anderson, 2004). The eastward-extended jet stream is a characteristic feature of the post-1977 climate regime (Trenberth and Hurrell, 1994). Due to a shorter distance between the trough and the ridge, the gradients in the 500-hPa height field are increased over the Northeast Pacific (Fig. 3D), which results in anomalous southeasterly flow.

Following the jet stream, cyclones move along the more southern trajectory and farther east and then curve northward to the Gulf of Alaska (Fig. 3E). The secondary storm track along the Siberian coast is practically absent. The southward excursion of the storm trajectories is also accompanied by strengthening of the westerly winds along approximately 30°N and their weakening within the 50°–60°N zone (Lau, 1988). In this state, storms bring warm air and moisture from the subtropical latitudes to Alaska and the west North American coast, known locally as the “Pineapple Express”.

The SAT anomaly pattern of Fig. 3F is characteristic of the positive phase of the PDO. An increased number of storms entering the eastern Bering Sea and the overall counterclockwise

Strong Aleutian low

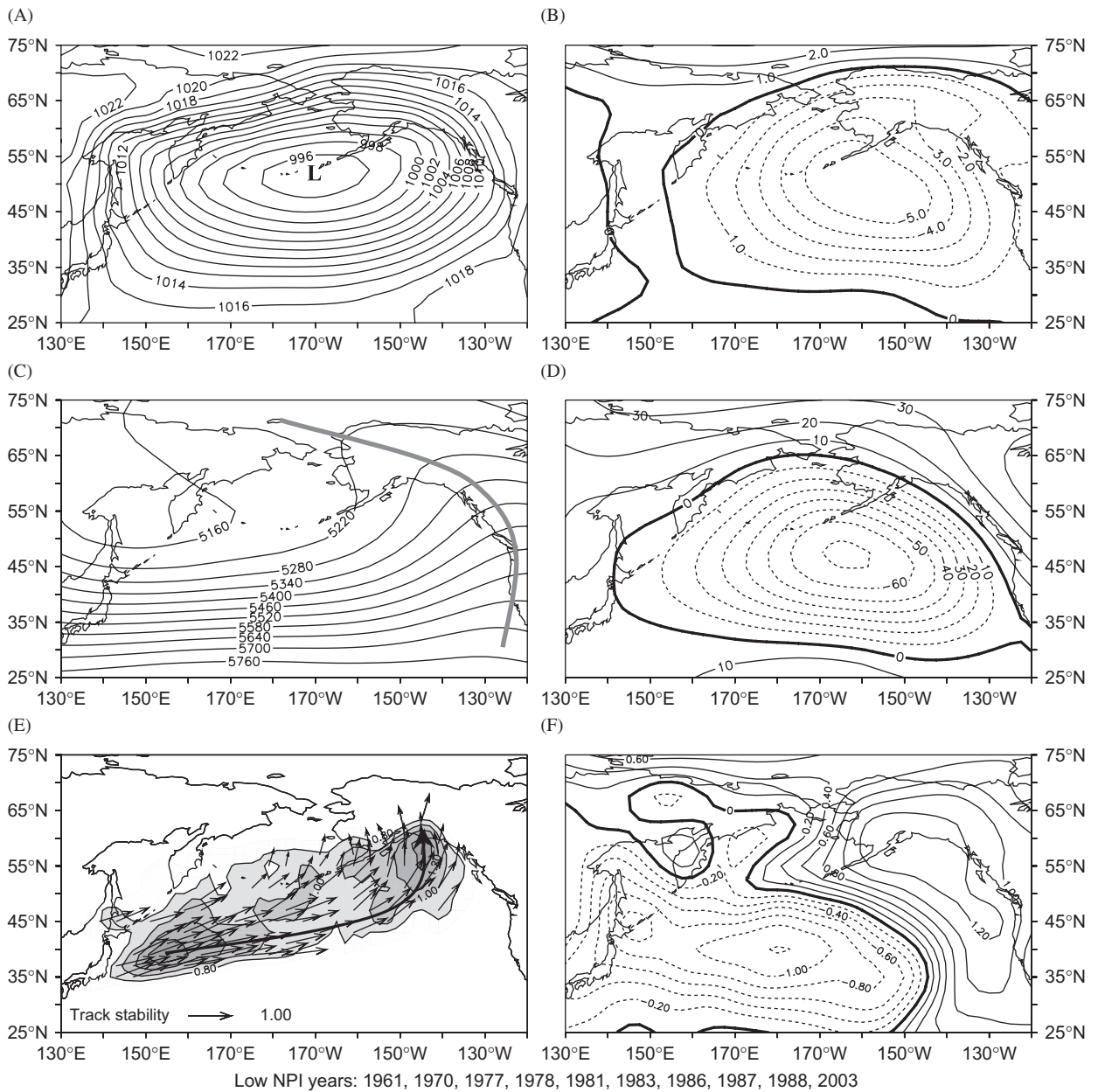


Fig. 3. Mean winter (DJFM) (A) SLP and (B) its anomaly, (C) 500-hPa height and (D) its anomaly, (E) storm track density (contours) and (F) SAT anomalies for 10 years with the strongest Aleutian Low (lowest NP index values) since 1950. The heavy gray line in the middle left panel and the arrows in the lower left panel are the same as in Figs. 1B and C, respectively. SAT anomalies are deviations from the 1951–2000 climatology normalized by the standard deviation in each grid point.

circulation anomalies increase the advection of warm Pacific air northward into Alaska and then westward to the Bering Sea. The eastern part of the Bering Sea is warmer than normal and the western part is slightly colder than normal.

When the Aleutian Low is weak (high NP index), it is often split into two centers, with one in the Northwest Pacific and the other in the Gulf of Alaska (Fig. 4A). The western center is somewhat stronger than the eastern one and is therefore often

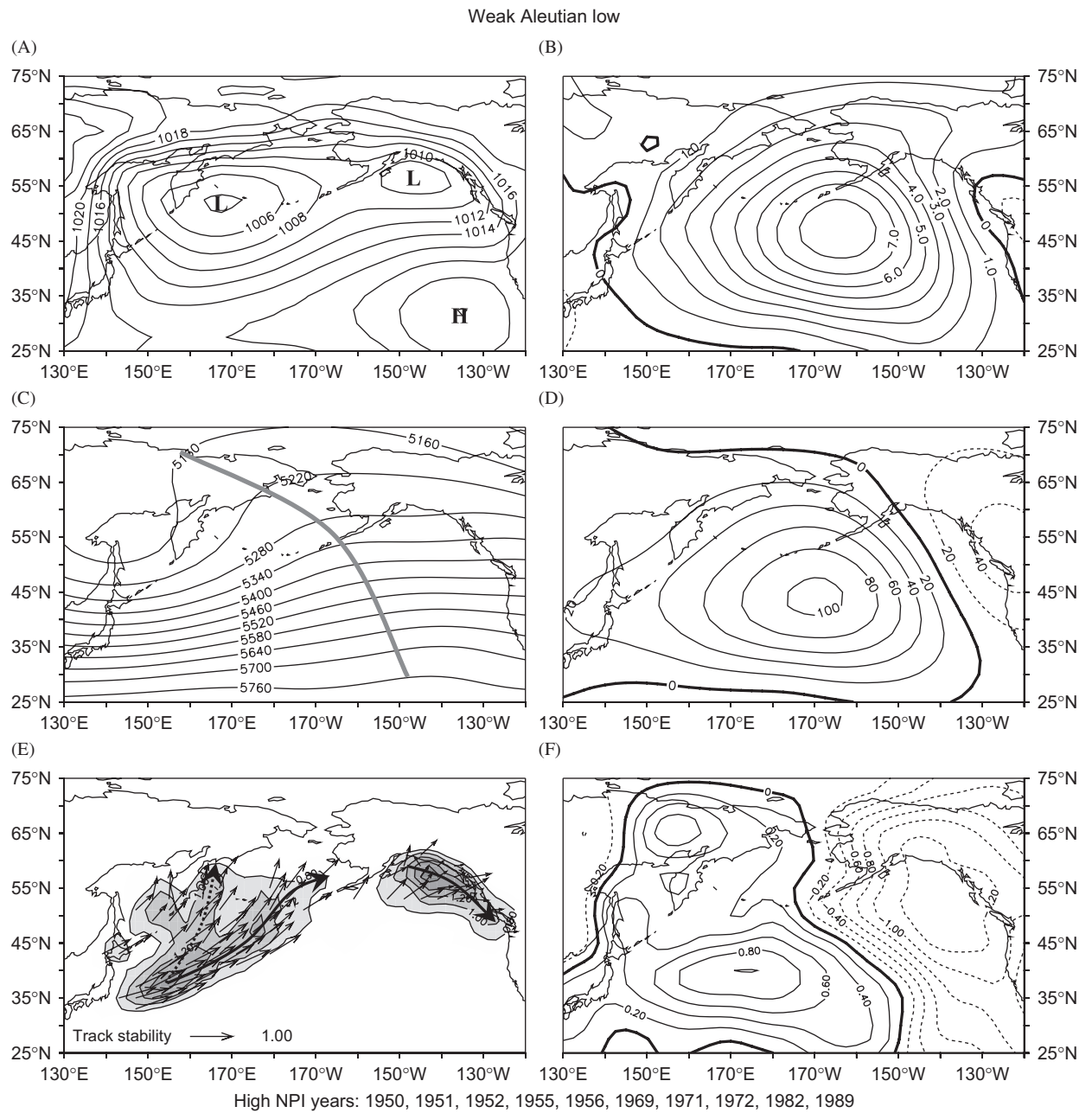


Fig. 4. Same as Fig. 3, except for 10 years with the weakest Aleutian Low (highest NP index values).

considered as the center of the Aleutian Low. The western center is located to the west of the long-term mean position of the Aleutian Low (see Fig. 1A), thus reinforcing the relationship between the strength of the Aleutian Low and its longitudinal position mentioned above. Note also that the Sub-tropical High is stronger than average and is shifted northward. The distribution of SLP anomalies

(Fig. 4B) features a high-pressure center south of the Alaska Peninsula, in the region of the primary North Pacific storm track. Overall, it is a mirror image of SLP anomalies in the case of a strong Aleutian Low (Fig. 3B). It is worth noting that, of the 10 cases that went into this composite, six coincide with La Niña events, and none with El Niño. The mid-tropospheric ridge that was over

the west North American coast in the case of a strong Aleutian Low is now shifted to the central North Pacific (cf. Figs. 3C and 4C). The 500-hPa geopotential height anomalies in this area are up to 100 m higher than normal (Fig. 4D). Bond and Harrison (2000) showed that, during periods when ridges form over the central North Pacific, anomalies in turbulent air–sea heat fluxes and low-level baroclinity associated with the PDO are manifested differently in their effects on transient eddies (storms) than during troughs. These effects may help to explain why prominent ridges occur about three times more frequently during periods when the PDO is significantly negative than when it is positive.

The anomalous mid-tropospheric ridge over the Central North Pacific obstructs, and at times, even blocks the normal west-to-east propagation of migratory cyclones. In Fig. 4E, the number of storms crossing the central North Pacific is reduced, and the primary storm track is shifted northward following the northward shift of the westerly jet stream (Lau, 1988). In the Gulf of Alaska, storms move southeastward more frequently in conjunction with anomalous troughing aloft.

The distribution of SAT anomalies over the North Pacific (Fig. 4F) represents a typical negative PDO pattern. The SAT anomalies in the Bering Sea change sign slightly east of 180° longitude, with positive anomalies in the western part and negative anomalies in the eastern part. This means that even minor variations in the position of the blocking ridge, and hence storm tracks, can cause SAT anomalies at St. Paul to switch sign.

3.4. “Warm” vs. “cold” winters in the Bering Sea

The list of months that went into the W1 and C1 composite patterns is presented in Table 1. The period 1950–1976, i.e. prior to the 1977 regime shift, included 16 months with W1 and 20 months with C1 types of atmospheric circulation. After the regime shift, from 1977 to 2002, the balance favored W1 (20 to 7). According to the chi-square test, the change in the ratio of W1 to C1 types is statistically significant at the 0.02 level.

The SLP map for the W1 type of atmospheric circulation, which is the most common pattern for anomalously warm winter months in the Bering Sea (Rodionov et al., 2005), features a strong, single-centered Aleutian Low with an average SLP of 996 hPa in its center (Fig. 5A), or about 5 hPa

Table 1
A list of months in the W1 and C1 composites

W1		C1	
Mar-50	Jan-79	Jan-51	Feb-76
Feb-51	Mar-80	Jan-54	Mar-76
Dec-51	Dec-83	Feb-56	Feb-84
Feb-55	Dec-84	Dec-56	Jan-86
Jan-57	Jan-85	Feb-57	Feb-91
Mar-58	Dec-85	Mar-59	Jan-93
Feb-59	Dec-86	Feb-61	Mar-95
Feb-60	Mar-87	Dec-61	Jan-98
Dec-60	Jan-88	Jan-62	Dec-99
Feb-62	Feb-89	Feb-65	
Jan-66	Dec-90	Jan-71	
Feb-66	Mar-91	Mar-71	
Mar-67	Mar-93	Feb-72	
Jan-68	Mar-96	Mar-72	
Jan-69	Feb-00	Jan-73	
Feb-70	Dec-00	Feb-74	
Jan-78	Feb-01	Dec-74	
Dec-78	Mar-02	Jan-75	

deeper than average (Fig. 5B). Although the Aleutian Low normally shifts southeastward when it strengthens (see previous section), in the case of W1 it shifts westward and northward of its normal position. This is consistent with the results of Luchin et al. (2002).

The 500-hPa height map (Fig. 5C) indicates that the eastern North Pacific ridge is relatively strong and shifted westward from its normal position, but not as much as in the case of high NP index values (Fig. 4C). The 500-hPa height anomaly map (Fig. 5D) features a west–east dipole positioned so that the Bering Sea experiences anomalous southerly geostrophic winds. This map closely resembles the composite 700 mb height-anomaly map from Overland et al. (2002) pertaining to anomalies in the net surface heat flux in January–March. Anomalous heating (cooling) tends to occur during periods of anomalous southerly (northerly) winds in association with suppressed (enhanced) surface fluxes of sensible and latent heat.

An important feature of W1 circulation type is the northward extension of the upper atmospheric ridge (over Alaska and the Gulf of Alaska), due to its relationship to transient storms. This is consistent with Fang and Wallace (1994), who showed that positive 500-hPa height anomalies over Alaska are related to negative sea ice anomalies in the Bering Sea. Due to this stronger and westward-shifted upper atmospheric ridge, storm activity along the primary storm track in

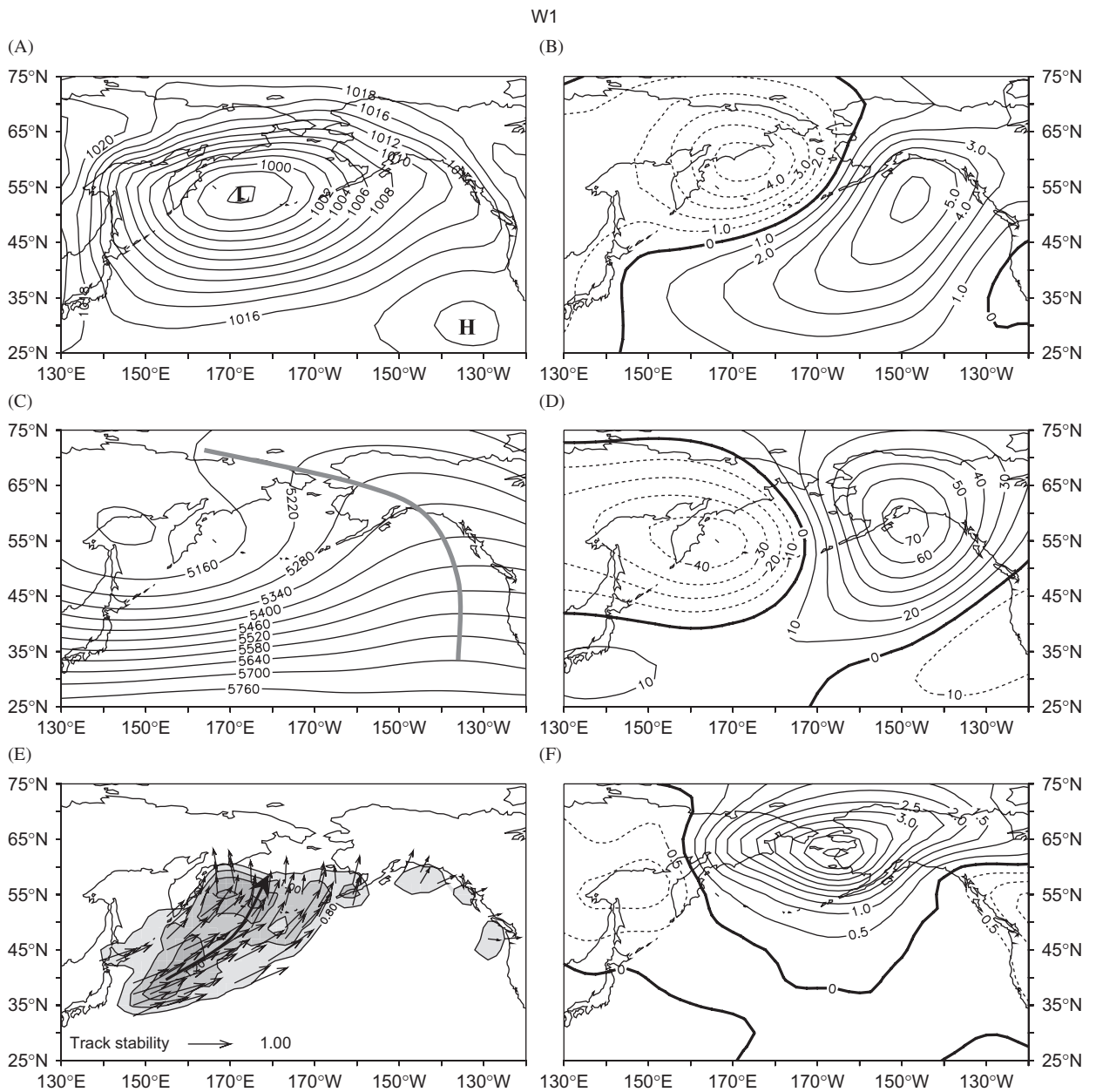


Fig. 5. Same as Fig. 3, except for W1 type of atmospheric circulation characteristic for anomalously warm winters in the Bering Sea (adapted from Rodionov et al., 2005).

the central and eastern North Pacific is suppressed and the majority of storms are steered into the Bering Sea along the secondary storm track off the Siberian coast (Fig. 5E), with similarities to the case of a weak Aleutian Low (Fig. 4E). An important difference between Fig. 4E and Fig. 5E is that the number of storms in the Gulf of Alaska in the latter case is greatly reduced.

The westward shift of the upper atmospheric ridge is particularly noticeable in its southern part over the eastern Pacific. This creates an anomalous northerly component of geostrophic winds over the North American west coast, and, as a result, negative SAT anomalies south of 60°N (Fig. 5F). Since the late 1970s, both the Bering Sea and the California Current system experienced a warm

climatic regime. In late 1998, however, the California Current switched to a colder regime, and its ecosystem responded with increased productivity and the return of subarctic species (Peterson and Schwing, 2003). At the same time, the Bering Sea continued to experience a warm regime, which has been beneficial for such major fisheries as walleye pollock (*Theragra chalcogramma*) and sockeye salmon (*Oncorhynchus nerka*).

The principal atmospheric circulation pattern for anomalously cold winters in the Bering Sea (type C1) is characterized by a split Aleutian Low (Fig. 6A), similar to the pattern for positive NP index values (Fig. 4A). An important difference between these two patterns is that the western center of low pressure in Fig. 6A is located farther south than in Fig. 4A. By definition of type C1 (Rodionov et al., 2005), the Aleutian Low should not only be

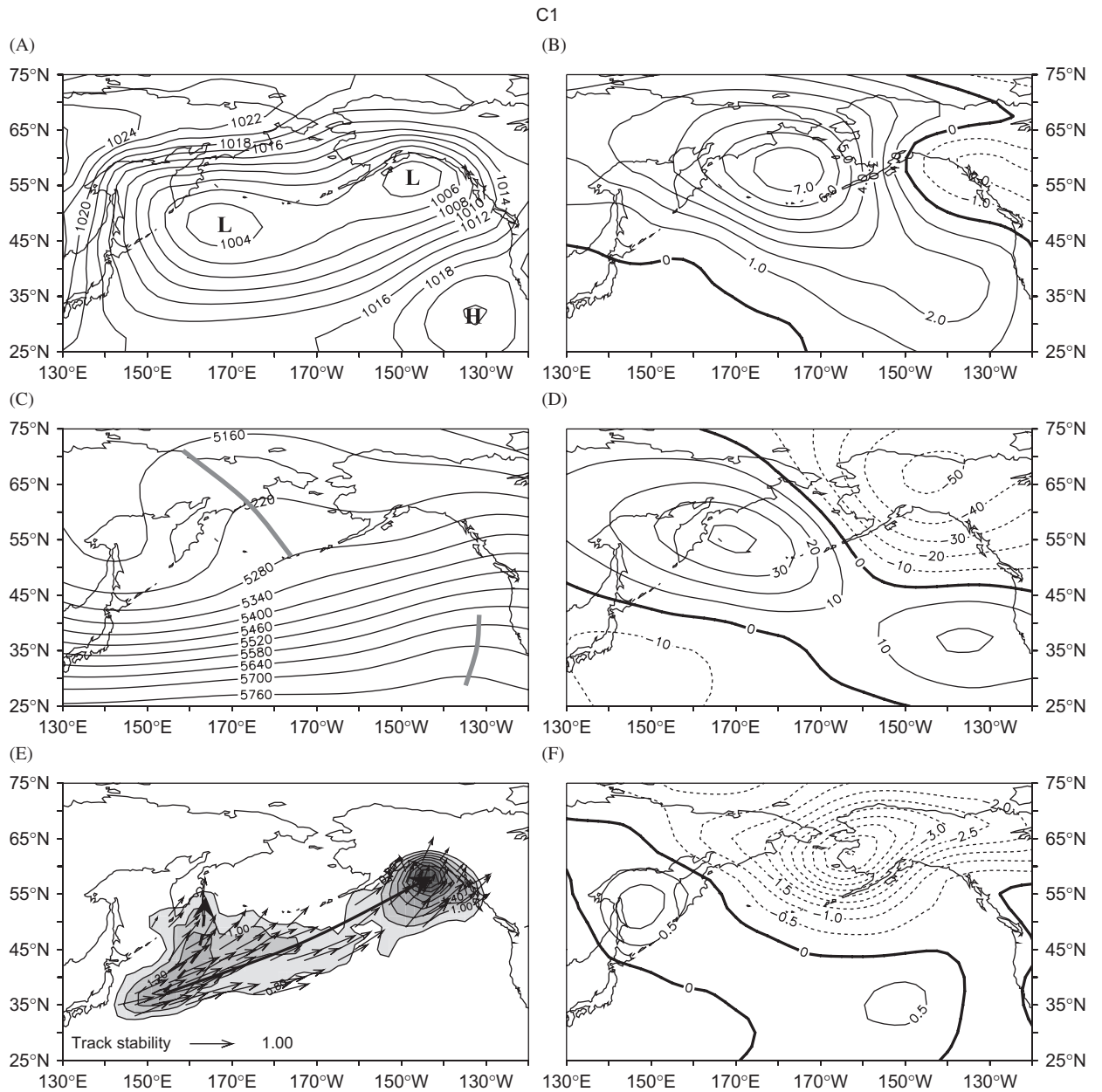


Fig. 6. Same as Fig. 3, except for C1 type of atmospheric circulation characteristic for anomalously cold winters in the Bering Sea (adapted from Rodionov et al., 2005).

split, but also its western center should be south of 52°N. It is important to note that this southward shift of the western center is accompanied by a stronger and eastward expansion of the Siberian High. This eastward extension of the Siberian High appears to be the primary cause of the positive SLP anomalies over the Bering Sea (Fig. 6B), as opposed to anomalies that appear to be of more North Pacific origin in the case of a weak Aleutian Low (Fig. 4B).

The mid-tropospheric circulation is characterized by a ridge over the Bering Sea and the eastern tip of Siberia (Fig. 6C), which is similar to the ridge in Fig. 4C, but shifted even more westward. In addition to this westward shift, another important difference between Figs. 4C and 6C is that in the latter case the ridging is absent in the mid-latitudes, where the mean zonal flow remains largely unobstructed. This is clearly seen in Fig. 6D, where 500-hPa anomalies along the primary storm track are relatively small. In other words, the ridge in type C1 is expressed at higher latitudes than its counterpart for the case of high NP index (Fig. 4C,D).

The lack of blocking in the mid-latitudes allows the storms cross the central North Pacific with near-normal frequency (Fig. 6E). The storm activity in the Gulf of Alaska is extremely high, which suggests enhanced local cyclogenesis. This is consistent with more frequent troughing aloft (Fig. 6D). The troughing, however, is not as deep as in the case of a weak Aleutian Low (Fig. 4D). A comparison of the shapes of storm density contours in the Gulf of Alaska in Figs. 4E and 6E shows that storms move southeastward along the North American west coast less frequently during C1 circulation patterns; instead, they continue northeastward. Although the secondary storm track in the Northwest Pacific is also active, the storms along the Siberian coast tend not to reach as far north as in W1 conditions. Their lack of penetration into the western Bering Sea is associated with anomalously high SLP over the eastern tip of Siberia. The anomalous northerly flow on the eastern periphery of the upper atmospheric ridge (Fig. 6C, D) implies enhanced transport of air of Arctic origin into the eastern Bering Sea and Alaska. As result, winter temperatures in those areas are well below normal (Fig. 6F).

3.5. Changes in Siberian and Alaskan storm tracks

As shown above, no statistically significant correlation exists between the NP index and winter

SAT at St. Paul. Therefore, the NP index (as well as other climatic indices related to the strength of the Aleutian Low, such as the PDO and PNA) is not a good diagnostic indicator of severity of any particular winter in the Bering Sea. For example, during the cold climate regime from 1940 to 1976, there were more anomalously cold winters accompanied by positive than by negative anomalies of the NP index (15 to 8). But there were also more anomalously warm winters during the same period accompanied by positive than by negative anomalies of the NP index (9 to 2). During the warm climate regime, 1977–2005, there were more anomalously warm winters in conjunction with the negative than with the positive NP index (12 to 6). But there were also more cold winters concurrently with the negative than with the positive NP index (7 to 3). The lack of overall correlation between the NP index and SAT at St. Paul poses an important question about the cause(s) of the increased frequency of anomalously warm winters in the Bering Sea since 1977, simultaneously with a shift toward a strong Aleutian Low regime.

It is reasonable to assume that the increased frequency of warm winters is more closely associated with changes in the storm tracks than with the overall strength of the Aleutian Low. In addition to W1, two other circulation patterns classified by Rodionov et al. (2005), namely W2 and W4, also feature a distinct Siberian storm track. In contrast, types W3 and W5 both represent a strong Aleutian Low with a well-defined Alaskan storm track, which is a slightly modified primary North Pacific storm track, when storms enter the eastern Bering Sea from the southeast (Fig. 7). To examine the temporal variability of storm frequency along these two tracks, we calculated the frequency of

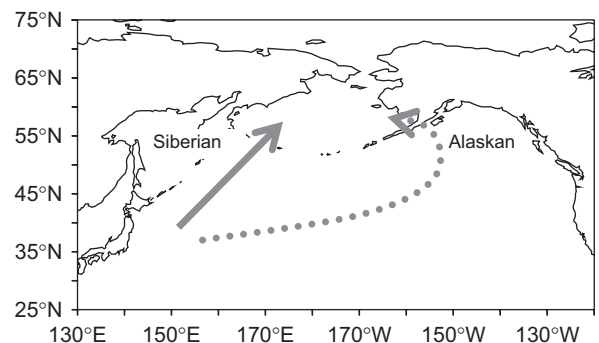


Fig. 7. Siberian and Alaskan storm tracks associated with anomalously warm winters in the Bering Sea.

Table 2

Average frequency (number of months per winter season, DJFM) of types W1 + W2 + W4, characterizing the Siberian storm track, and W3 + W5, characterizing the Alaskan storm track, and the percentage of Alaskan storm tracks

Period	Siberian	Alaskan	% Alaskan
1916–2005	0.83	0.38	31
1922–1939	0.89	0.72	45
1940–1976	0.76	0.05	7
1977–2005	0.96	0.66	40

types W1 + W2 + W4 and W3 + W5 for the entire period of observations, 1916–2005, and separately for each warm (1922–1939 and 1977–2005) and cold (1940–1976) regime in the Bering Sea (Table 2). For the period 1916–2005, there were in total 124 anomalously warm winter months in the Bering Sea, 109 of which (or 89%) were associated with the types W1–W5. The remaining 15 months (or 11%) were misclassified, and, for simplicity, we considered them as being associated with storm tracks other than Siberian or Alaskan, and removed them from further analysis. Their exclusion does not affect the main conclusion of this analysis.

Table 2 shows that, for the entire period of observations, the Alaskan storm track accounts for about one-third of cases with anomalously warm winter months. During the warm regimes, however, the portion of storms entering the Bering Sea along the Alaskan track increased to 45% in 1922–1939 and 40% in 1977–2005. In contrast, during the cold regime of 1940–1976, this portion dropped to a mere 7%. It is not surprising, therefore, that Overland and Pease (1982), who worked mostly with the data prior to the 1977 regime shift, found little evidence of anomalously warm winters in the Bering Sea in association with the Alaskan storm track. During the cold regime, even in the years when the Aleutian Low is strong, most storms, instead of entering the Bering Sea, propagate northward over interior Alaska. In these situations, north winds occur over the eastern Bering Sea, promoting ice development and advance.

It is important to underscore that the frequency of patterns with storms entering the Bering Sea along the Siberian track is relatively stable over time, while the frequency of the patterns with storms along the Alaskan track can change dramatically from one climatic regime to another. Although the number of anomalously warm months

associated with the Siberian storm track somewhat increases during warm climate regimes, it is the Alaskan storms track activity that makes much of the difference between the warm and cold climate regimes in the Bering Sea.

3.6. Two types of northerly winds

Although there is practically no correlation between the year-to-year variations in the NP index and SAT at St. Paul, there is a relatively strong correlation between the NP index and northerly winds over the eastern Bering Sea. For the period 1949–2005, the correlation coefficient between the mean winter (DJFM) NP index and the meridional component of surface wind at St. Paul is $r = -0.54$, which is statistically significant at the 99% level. The northerly winds, in turn, are almost equally strongly correlated with SAT at St. Paul ($r = -0.53$ for the same period). Based on these correlation coefficients, one might assume that, in the case of a strong Aleutian Low, there would be a tendency toward stronger northerly winds, and, hence, colder temperatures in the eastern Bering Sea. From this, the shift to the regime of a strong Aleutian Low in 1977 should have resulted in a colder climate for the eastern Bering Sea. As is well known, the opposite has happened. This is another inconsistency in the relationship between the Aleutian Low and Bering Sea climate.

Sasaki and Minobe (2005) note that a single mode is not sufficient to explain the relationship between the sea ice concentration and wind anomalies in the Bering Sea, but at least two modes should be taken into account. According to their singular value decomposition analysis, the first mode of sea ice variation in the winter and spring seasons is related to large-scale atmospheric circulation associated with the Aleutian Low and the second mode is related to relatively local atmospheric fluctuations associated with pressure anomalies over Alaska. Our analysis suggests that the second mode appears to be linked more to pressure anomalies over northeast Siberia, which is one of the centers of anticyclogenesis and frequency maxima in winter (Bell and Bosart, 1989).

Fig. 8 shows SLP anomaly distributions for the winters of 1975 and 2003, illustrating two types of northerly winds. The anomalously cold winter of 1975 had strong northerly winds over the Bering Sea caused by persistently high SLP over northeastern Siberia (McLain and Favorite, 1976). The advection

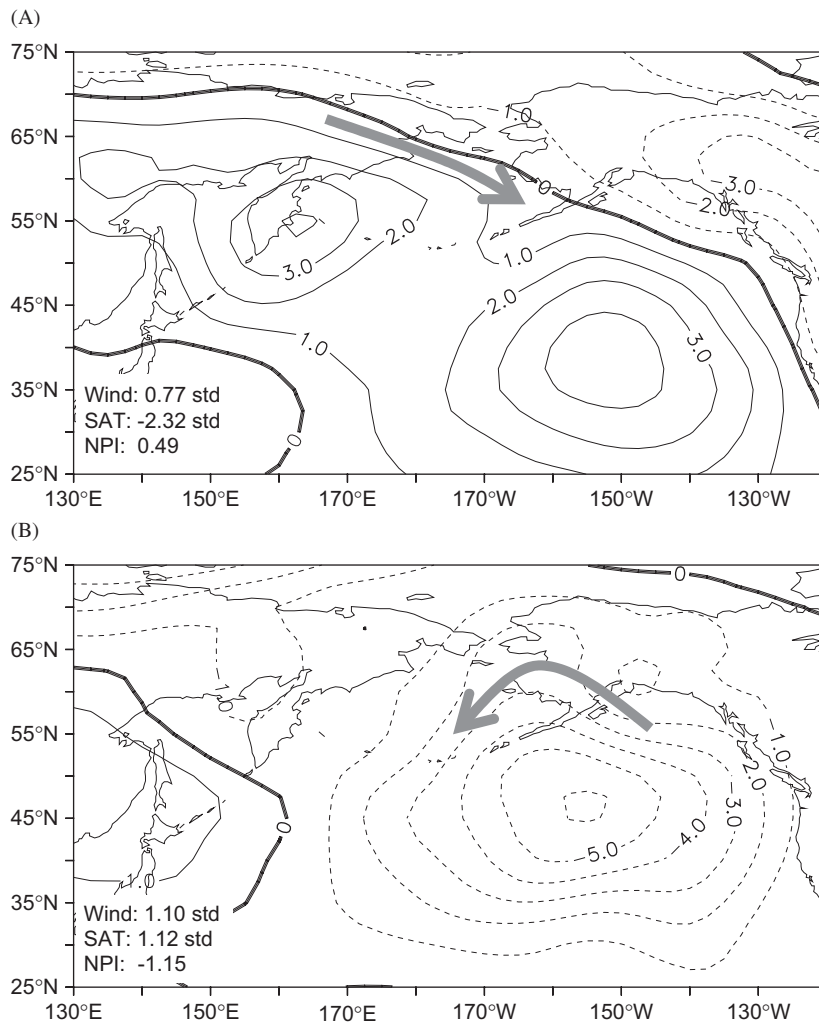


Fig. 8. SLP anomalies in the winters (DJFM) of (A) 1975 and (B) 2003 illustrating two types of anomalous northerly wind component over the Bering Sea.

of cold and dry Siberian and Arctic air resulted in enhanced heat loss by the sea through sensible and latent heat fluxes into the atmosphere, which accelerated ice formation and its expansion southward. An extensive ice cover shut down the ocean–atmosphere heat exchange and cooled the air even further. When ice reached the Pribilof Islands, SAT at St. Paul dropped precipitously.

During the winter of 2003 (Fig. 8B), the northerly winds over the Bering Sea were even stronger than in 1975. Nevertheless, positive SAT anomalies at St. Paul exceeded one standard deviation, and the winter was ranked as the 12th warmest on record since 1916. These northerly winds were associated with an enhanced cyclonic activity south of the

Alaska Peninsula. In this case, winds over the southeastern Bering Sea transported the modified Pacific air that was previously pumped into Alaska by frequent storms. The effects of these winds on thermal conditions in the Bering Sea were twofold. On the one hand, they accelerated the conveyor belt of ice formation in polynyas and its advancement to the south. Also, the stronger the wind, the faster the cooling of the sea, given all other conditions equal. On the other hand, since this air was relatively warm and moist, the sensible and latent heat flux from the sea to the atmosphere was much less intense than under northerly winds of the same speed, but for cold and dry Arctic air masses. Note also that the zonal wind component of the wind created an

Table 3
Correlation coefficients for mean winter (DJFM) SAT and NP index with the northerly winds at St. Paul

Period	SAT	NP index
1949–1976	−0.71	−0.55
1977–2005	−0.48	−0.63
NPI < 0 (27 yr)	−0.48	−0.43
NPI > 0 (30 yr)	−0.80	−0.40

anomalous Ekman transport northward in 2003 and southward in 1975.

The situations like that in the winter of 2003 reduce the strength of correlation between the northerly winds and SAT at St. Paul. The probability of such situations increases during the regimes of a strong Aleutian Low, which explains why the correlation coefficient between the northerly winds and SAT reduces from −0.71 to −0.48 between the periods 1949–1976 and 1977–2005 (Table 3). The difference in the correlation coefficients is even more substantial between two groups of years partitioned by the NP index (−0.80 for positive versus −0.48 for negative NP index values); this difference is statistically significant at the 95% confidence level.

It is interesting to note that while the correlation between the NP index and northerly winds is quite strong for the ongoing warm regime, 1977–2005 (Table 3), it has changed significantly between the beginning of the regime and more recent years. For the period 1977–1989 the correlation is strong ($r = -0.89$), while for the period 1990–2005 this correlation is weak ($r = -0.22$). This can be explained by a tendency of maximum storm activity to have occurred farther west and north in the earlier years of the regime, so that the Bering Sea was often on the eastern periphery of the Aleutian Low, and hence subject to southerly winds. Recently, there has been an increased occurrence of winters with negative NP index values (strong Aleutian Lows) coinciding with positive SAT anomalies but inconsistent wind anomalies, thus reducing the strength of the correlation.

4. Summary

The effect of the Aleutian Low on Bering Sea winter climate is more complex than previously appreciated. In the North Pacific, shifts from one multidecadal PDO regime to another are associated

with the corresponding shifts in the *strength* of the Aleutian Low. Although the Bering Sea climate clearly responds to these shifts, its year-to-year variability is determined primarily by the *position* of the Aleutian Low and the corresponding storm tracks.

Anomalous warm winters in the Bering Sea are associated primarily with enhanced cyclonic activity along the Siberian storm track, which is a secondary storm track of the North Pacific. In addition, warm winters in the Bering Sea can also be associated with an active Alaskan storm track, which represents a primary storm track for the North Pacific. The frequency of storms along the Siberian track is independent of the decadal-scale climate regime in the North Pacific. In contrast the frequency of storms along the Alaskan track increases dramatically during the climate regimes of a strong Aleutian Low, thus increasing the overall probability of anomalously warm winters in the Bering Sea. It should be emphasized that even during those climate regimes the majority of mild winters in the Bering Sea are still associated with the Siberian storm track, but those additional mild winters that are associated with the Alaskan storm track shift the balance of winters, which results in a warmer climate regime in the Bering Sea.

There are four major climate states in the relationship between the Aleutian Low and Bering Sea climate:

State 1: A strong Aleutian Low is located somewhat east of its long-term mean position. The upper atmospheric ridge is positioned over the North American west coast. Storms tend to move across the central Pacific along southern paths and then turn sharply north into the Gulf of Alaska. Whether they enter the Bering Sea (which results in a mild winter), or continue northward (which results in a cold winter), depends on small variations in the position of the North American ridge and whether or not it extends all the way to Alaska.

State 2: The Aleutian Low is stronger than average, but shifted westward and northward compared to State 1. The upper atmospheric ridge is also shifted west, particularly its southern part, which is now over the eastern Pacific instead of the west coast of North America. Most of the storms are steered into the Bering Sea, resulting in temperatures well above normal.

State 3: An anomalous upper atmospheric ridge is located farther west toward the central Pacific, and there is suppression of storm activity in the central

North Pacific. The Aleutian Low is weak and often split into two centers. The secondary North Pacific storm track along the Siberian coast is active, but minor variations in the position of the blocking ridge determine whether the storms are steered into the Bering Sea or farther west. Similarly, they determine whether or not the area affected by the advection of cold Arctic air along the eastern periphery of the ridge will include the eastern Bering Sea.

State 4: The Aleutian Low is still weak, but the atmospheric flow in the middle latitudes is relatively zonal. Cyclones typically track across the North Pacific just south of the Aleutian Islands. Anomalous high-pressure cells dominate over northeastern Siberia. Due to the anticyclonic circulation, the Bering Sea experiences an enhanced advection of cold and dry Arctic air. This situation is characteristic of the coldest years in the Bering Sea.

The change between states is not necessarily in the order described above. States 1 and 3 represent the classical positive and negative PNA/PDO states, respectively. During these states, the Bering Sea is almost equally likely to be anomalously cold or warm. States 2 and 4 represent the primary states for warm and cold winters in the Bering Sea, respectively. They are associated with changes in the position of the Aleutian Low (and storm tracks), but not with its strength. Therefore, the PDO, NP and other indices of North Pacific climate, which reflect the strength of the Aleutian Low, are poor indicators of the severity of any individual winter in the Bering Sea.

There are two types of northerly winds in the Bering Sea, differing in their effect on air temperatures. During positive PDO regimes, the northerly winds over the Bering Sea are often associated with a strong Aleutian Low, and their effects on temperatures are modest. Conversely, during negative PDO regimes, when the Aleutian Low is weak, the correspondence between northerly winds and air temperatures in the Bering Sea is very strong.

Acknowledgments

We thank two anonymous reviewers for their detailed comments and suggestions. This publication is funded by the Joint Institute for the Study of the Atmosphere and Ocean (JISAO) under NOAA Cooperative Agreement No. NA17RJ1232, Contribution No. 1243, and represents NOAA's Pacific Marine Environmental Laboratory Contribution

No. 2862, and Fisheries-Oceanography Coordinated Investigations (FOCI) contribution No. 0572. We appreciate the support of the NOAA Arctic Research Office and North Pacific Climate Regimes and Ecosystem Productivity (NPCREP)/FOCI programs. This paper was first presented in the GLOBEC-ESSAS Symposium on "Effects of climate variability on sub-arctic marine ecosystems", hosted by PICES in Victoria, BC, May 2005.

References

- Anderson, B.T., 2004. Investigation of a large-scale mode of ocean-atmosphere variability and its relation to tropical Pacific sea surface temperature anomalies. *Journal of Climate* 17, 4089–4098.
- Bell, G.D., Bosart, L.F., 1989. 15-year climatology of Northern Hemisphere 500 mb closed cyclone and anticyclone centers. *Monthly Weather Review* 117, 2142–2163.
- Bond, N.A., Harrison, D.E., 2000. The Pacific Decadal Oscillation, air-sea interaction and central north Pacific winter atmospheric regimes. *Geophysical Research Letters* 27, 731–734.
- Fang, Z., Wallace, J.M.J., 1994. Arctic sea ice variability on a time scale of weeks and its relation to atmospheric forcing. *Journal of Climate* 7, 1897–1914.
- Gulev, S.K., Zolina, O., Grigoriev, S., 2001. Extratropical cyclone variability in the Northern Hemisphere winter from the NCEP/NCAR reanalysis data. *Climate Dynamics* 17, 795–809.
- Gyakum, J.R., Anderson, J.R., Gru, E.L., 1989. North Pacific cold-season surface cyclone activity: 1975–1983. *Monthly Weather Review* 117, 1141–1155.
- Hayden, B.P., 1981a. Cyclone occurrence mapping: equal area or raw frequencies? *Monthly Weather Review* 109, 168–172.
- Hayden, B.P., 1981b. Secular variation in Atlantic Coast extratropical cyclones. *Monthly Weather Review* 109, 159–167.
- Hoskins, B.J.A., Valdes, P.J., 1990. On the existence of storm-tracks. *Journal of the Atmospheric Sciences* 47, 1854–1864.
- Kalnay, E., Kanamitsu, M., Kistler, R., Collins, W., Deaven, D., Gandin, L., Iredell, M., Saha, S., White, G., Woollen, J., Zhu, Y., Chelliah, M., Ebisuzaki, W., Higgins, W., Janowiak, J., Mo, K.C., Ropelewski, C., Wang, J., Leetmaa, A., Reynolds, R., Jenne, R., Joseph, D., 1996. The NCEP/NCAR 40-year reanalysis project. *Bulletin of the American Meteorological Society* 77, 437–471.
- Lau, N.-C., 1988. Variability of the observed midlatitude storm tracks in relation to low-frequency changes in the circulation pattern. *Journal of the Atmospheric Sciences* 45, 2718–2743.
- Luchin, V.A., Semiletov, I.P., Weller, G.E., 2002. Changes in the Bering Sea region: atmosphere-ice-water system in the second half of the twentieth century. *Progress in Oceanography* 55, 23–44.
- Mantua, N.J., Hare, S.R., Zhang, Y., Wallace, J.M., Francis, R.C., 1997. A Pacific interdecadal climate oscillation with impacts on salmon production. *Bulletin of the American Meteorological Society* 78, 1069–1079.

- McLain, D.R., Favorite, F., 1976. Anomalously cold winters in the southeastern Bering Sea, 1971–75. *Marine Science Communications* 2, 299–334.
- Mock, C.J., Patrick, J.B., 1998. Atmospheric circulation patterns and spatial climatic variations in Beringia. *International Journal of Climatology* 18, 1085–1104.
- Niebauer, H.J., 1983. Multi-year sea ice variability in the eastern Bering Sea: an update. *Journal of Geophysical Research* 88, 2733–2742.
- Niebauer, H.J., 1988. Effects of El Niño-Southern Oscillation and North Pacific weather patterns on interannual variability in the subarctic Bering Sea. *Journal of Geophysical Research* 93, 5051–5068.
- Niebauer, H.J., 1998. Variability in Bering Sea ice cover as affected by a regime shift in the Pacific in the period 1947–1996. *Journal of Geophysical Research* 103, 27717–27737.
- Niebauer, H.J., Bond, N.A., Plotnikov, V.V., 1999. An update on the climatology and sea ice of the Bering Sea. In: Loughlin, T.R., Ohtani, K. (Eds.), *Dynamics of the Bering Sea*. University of Alaska Sea Grant, Fairbanks, Alaska, pp. 29–60.
- Overland, J.E., Pease, C.H., 1982. Cyclone climatology of the Bering Sea and its relation to sea ice extent. *Monthly Weather Review* 110, 5–13.
- Overland, J.E., Adams, J.M., Bond, N.A., 1999. Decadal variability of the Aleutian Low and its relation to high-latitude circulation. *Journal of Climate* 12, 1542–1548.
- Overland, J.E., Bond, N.A., Adams, J.M., 2002. The relation of surface forcing of the Bering Sea to large-scale climate patterns. *Deep-Sea Research* 49, 5855–5868.
- Peterson, W.T., Schwing, F.B., 2003. A new climate regime in Northeast Pacific ecosystems. *Geophysical Research Letters* 30, 1896.
- Rodionov, S., 2004. A sequential algorithm for testing climate regime shifts. *Geophysical Research Letters*, 31 (L09204).
- Rodionov, S.N., Overland, J.E., Bond, N.A., 2005. The Aleutian low and winter climatic conditions in the Bering Sea. Part I: Classification. *Journal of Climate* 18, 160–177.
- Rogers, J.C., 1981. The north Pacific oscillation. *Journal of Climatology* 1, 39–57.
- Sasaki, Y.N., Minobe, S., 2005. Seasonally dependent inter-annual variability of sea ice in the Bering Sea and its relation to atmospheric fluctuations. *Journal of Geophysical Research* 110, C05011.
- Serreze, M.C., 1995. Climatological aspects of cyclone development and decay in the Arctic. *Atmosphere–Ocean* 33, 1–23.
- Serreze, M.C., Carse, F., Barry, R.G., Rogers, J.C., 1997. Icelandic low cyclone activity: climatological features, linkages with the NAO and relationships with recent changes in the Northern Hemisphere circulation. *Journal of Climate* 10, 453–464.
- Stabeno, P.J., Bond, N.A., Kachel, N.B., Salo, S.A., Schumacher, J.D., 2001. On the temporal variability of the physical environment over the southeastern Bering Sea. *Fisheries Oceanography* 10, 81–98.
- Taylor, K.E., 1986. An analysis of the biases in traditional cyclone frequency maps. *Monthly Weather Review* 114, 1481–1490.
- Trenberth, K.E., Hurrell, J.W., 1994. Decadal atmosphere–ocean variations in the Pacific. *Climate Dynamics* 9, 303–319.
- Wooster, W.S., Hollowed, A.B., 1995. Decadal-scale variations in the eastern subarctic Pacific: I. Winter ocean conditions. In: Beamish, R.J. (Ed.), *Climate Change and Northern Fish Populations*. Canadian Special Publication of Fisheries and Aquatic Sciences 121, National Research Council of Canada, Ottawa, pp. 81–85.
- Zolina, O., Gulev, S.K., 2002. Improving the accuracy of mapping cyclone numbers and frequencies. *Monthly Weather Review* 130, 748–759.